

RESEARCH

Open Access



Circulating miR-320a-3p and miR-483-5p level associated with pharmacokinetic–pharmacodynamic profiles of rivaroxaban

Hanxu Zhang^{1,2}, Zhuo Zhang¹, Zhiyan Liu¹, Guangyan Mu¹, Qiufen Xie¹, Shuang Zhou^{1,2}, Zhe Wang¹, Yu Cao³, Yunlong Tan⁴, Xiaohua Wei⁵, Dongdong Yuan⁶, Qian Xiang^{1*} and Yimin Cui^{1,2,7*}

Abstract

Background: Novel biomarkers for personalizing anticoagulation remain undetermined. We aimed to investigate the association of plasma miRNAs with pharmacokinetic–pharmacodynamic (PK-PD) profiles of rivaroxaban.

Methods: This is a multicenter, exploratory study of miRNAs in a Chinese population. Healthy volunteers and patients receiving rivaroxaban were enrolled in the study. The area under the plasma concentration–time curve from time 0–t h (AUC_{0-t}) and anti-Xa activity at 3 h (AXA_{3h}) were measured in healthy volunteers, and AXA_{3h} was measured in patients. MiRNAs were detected by miRNA microarray in 26 healthy volunteers with 20 mg rivaroxaban, and quantitative reverse transcription polymerase chain reaction was used to exclude undetectable ones. MiR-320a-3p and miR-483-5p were then quantified in 65 healthy volunteers and 71 patients. MiRNA levels at 3 h were compared between high and low AXA_{3h} or AUC_{0-t} subjects and in matched patients with or without bleeding during follow-up. The miRNA targets were predicted by TargetScan, miRtarBase, and miRDB. Validated genes were included in GO enrichment and KEGG analyses. The protein–protein interaction network was established by STRING and visualized by Cytoscape.

Results: A total of 136 Chinese subjects completed the study. In healthy volunteers taking 15 mg rivaroxaban, the miR-320a level at 3 h was significantly positively correlated with AXA_{3h} and AUC_{0-t} ($r=0.359$, $p=0.025$; $r=0.370$, $p=0.02$, respectively). A positive correlation was also observed between miR-483 and AXA_{3h} or AUC_{0-t} ($r=0.372$, $p=0.02$; $r=0.523$, $p=0.001$, respectively). MiR-320a and miR-483 levels at 3 h in the higher AUC_{0-t} group were significantly higher than those at 0 h. MiR-483 levels at 3 h may distinguish healthy volunteers with high or low AXA_{3h} or AUC_{0-t} . In the 10 mg fed subgroup, higher 3 h miR-483 levels were also observed compared with the control group. No significant differences were found in the comparisons among patients. Bioinformatic analysis showed that these miRNAs may play a regulatory role by targeting ABCG2, ITGB3, PTEN, MAPK1/3, etc.

Conclusions: MiR-320a and miR-483 levels were found to be associated with PK and PD profiles of rivaroxaban in healthy Chinese subjects. Further studies are required to verify these findings and explore the mechanisms.

Keywords: Circulating microRNA, Rivaroxaban, Pharmacokinetics, Pharmacodynamics

Background

Thromboembolic diseases are widespread and associated with high morbidity and mortality rates. Therefore, the prevention and treatment of thromboembolic disorders is of great importance. The routine use of direct

*Correspondence: xiangqz@pkufh.com; cui.pharm@pkufh.com

¹ Department of Pharmacy, Peking University First Hospital, No. 8, Xishiku Street, Xicheng District, Beijing 100034, China
Full list of author information is available at the end of the article



© The Author(s) 2022. **Open Access** This article is licensed under a Creative Commons Attribution 4.0 International License, which permits use, sharing, adaptation, distribution and reproduction in any medium or format, as long as you give appropriate credit to the original author(s) and the source, provide a link to the Creative Commons licence, and indicate if changes were made. The images or other third party material in this article are included in the article's Creative Commons licence, unless indicated otherwise in a credit line to the material. If material is not included in the article's Creative Commons licence and your intended use is not permitted by statutory regulation or exceeds the permitted use, you will need to obtain permission directly from the copyright holder. To view a copy of this licence, visit <http://creativecommons.org/licenses/by/4.0/>. The Creative Commons Public Domain Dedication waiver (<http://creativecommons.org/publicdomain/zero/1.0/>) applies to the data made available in this article, unless otherwise stated in a credit line to the data.

oral anticoagulants (DOACs) is a major breakthrough in the management of thromboembolic diseases [1]. Compared with vitamin K antagonists, DOACs have predictable pharmacokinetic (PK) and pharmacodynamic (PD) profiles, low potential for drug interaction, and are administered at fixed doses without the need for regular monitoring [2].

Rivaroxaban, an oral direct factor Xa inhibitor, is a DOAC that has been approved for clinical use in several thromboembolic disorders, such as stroke prevention in patients with nonvalvular atrial fibrillation and prevention or treatment of venous thromboembolism (VTE) [3]. Rivaroxaban is absorbed rapidly, with maximum concentrations (C_{max}) appearing 2 to 4 h after intake. The maximum factor Xa (FXa) inhibition is also reached 3 h after dosing [4, 5]. Oral bioavailability is high (80–100%) for the 10 mg tablet and is not affected by food. However, 15 mg and 20 mg tablets should be taken with food since coadministration with food can increase the area under the plasma concentration–time curve (AUC) and C_{max} [6]. A number of studies have confirmed that anti-Factor Xa chromogenic assays calibrated by rivaroxaban are best suited for the quantitative measurement of rivaroxaban plasma levels [7].

However, inter-individual variability in pharmacokinetic and pharmacodynamic parameters has been reported in healthy subjects and patients taking rivaroxaban [8, 9]. Changes in pharmacokinetics are expected to alter pharmacodynamics, which can cause drug toxicity or therapeutic failure. Therefore, biomarkers that can predict the PK and PD properties of rivaroxaban could help achieve the desired therapeutic drug effects and avoid bleeding in clinical drug therapy. Many genetic and non-genetic factors have been studied to determine whether they could contribute to this variability. However, the influence of genetic factors on clinical significance is inconsistent and based on limited research [10]. Moreover, biomarkers for predicting the PK and PD parameters of rivaroxaban are still lacking.

MicroRNAs (miRNAs), which are small non-coding RNAs with average lengths of 22 nucleotides, exist stably in various biofluids, including serum, plasma, and urine [11], and act as gene regulators [12]. A variety of miRNAs play a role in thrombosis and may act as biomarkers for thrombotic disease and a wide range of cardiovascular diseases such as atrial fibrillation, myocardial infarction, heart failure, atherosclerosis, hypertension, and type 2 diabetes mellitus [13–15]. It is also well recognized that miRNAs could be significant factors in the regulation of drug transporters and drug-metabolizing enzymes, and they may affect inter- and intra-individual variations in drug metabolism and disposition [16, 17]. Therefore, miRNAs may be associated with the PK-PD

profiles of rivaroxaban, which are metabolized by several cytochrome P450 enzymes (CYP3A4/5, CYP2J2) and excreted by P-glycoprotein (P-gp) and breast cancer resistance protein (BCRP) [6]. The levels of miRNAs may have the potential to distinguish subjects with different drug responses and help personalize pharmacotherapy. To date, no study has explored the association between miRNAs and PK-PD profiles of DOACs, which may be important and instructive. Thus, the purpose of this study was to investigate the correlation between plasma miRNAs and PK-PD profiles of rivaroxaban in healthy subjects and to determine their relationship in patients.

Methods

Settings and ethics statement

This is a multicenter, exploratory study of miRNAs in a Chinese population. Healthy volunteers and patients receiving rivaroxaban were enrolled in the study. The inclusion criteria are listed in the Additional file 1: Table S1. The study was conducted in accordance with the Good Clinical Practice guidelines and the Declaration of Helsinki. The protocol was approved by an independent ethics committee, the Institutional Review Board of Peking University First Hospital, and all participating research sub-central hospitals. All subjects signed an informed consent form. The trial registration number is NCT03161496.

Healthy volunteers received a single dose of rivaroxaban (10, 15, or 20 mg) under either fasted or fed conditions. In the fasted state, rivaroxaban was administered with water in the morning following an overnight fast (10 h). In the fed state, rivaroxaban was administered within 30 min after consumption of a standard high-fat, high-calorie breakfast.

Baseline characteristics of the patients were recorded when they were enrolled. The incidence of bleeding events was recorded at 1, 6, and 12 months after administration by telephone or at an outpatient clinic. If the patient was not followed up at 12 months, data were obtained using the last observation carried forward (LOCF) method.

Plasma collection

PK parameters were detected only in healthy volunteers, while PD parameters were detected in both healthy volunteers and patients. To detect PK parameters, venous blood samples (6 mL) were collected in 3.0/4.0 mL heparinized or EDTA-K2 tubes pre-dose and at 16–19 time points after drug administration. Blood samples were centrifuged at 4 °C for 10 min at 3000g within 120 min of sampling. To detect PD parameters, blood samples were collected in 2.7 mL sodium citrate (3.2% v/v) tubes at baseline and 3 h after administration (which was

considered the time to peak [18]). They were then centrifuged at room temperature for 15 min at 2500g within 60 min of sampling. To detect miRNA profiles, 6 mL of peripheral blood was collected in EDTA-2 K tubes at baseline and 3 h in healthy volunteers, and at 3 h in patients. The samples were centrifuged at 3000g and 4 °C for 10 min.

All plasma samples were immediately stored at −80 °C until analysis. PK assessment was conducted in each sub-center, and no significant matrix effect was found. Detailed PK assessment methods are shown in Additional file 2: Table S2. PD and miRNA assessments were performed at a centralized facility in the Peking University First Hospital.

PK, and PD analysis

PK parameters were determined by standard non-compartmental methods using Phoenix WinNonlin 7.0, (Pharsight Corporation, Sunnyvale, CA, USA) or DAS for EDC V5.0 (Medbanks, Beijing, China). The AUC from time 0-t h (AUC_{0-t}) was calculated using the linear trapezoidal rule.

The PD parameter, anti-FXa activity (AXA) of rivaroxaban, was measured using a validated chromogenic anti-FXa kit (BIOPHEN DiXaI[®], HYPHEN BioMed, Neuville sur Oise, France) with rivaroxaban calibrators and controls (BIOPHEN Rivaroxaban[®] Calibrator and Control, HYPHEN BioMed, Neuville sur Oise, France). AXA levels were determined using a Sysmex[®] CS2100i (Sysmex, Kobe, Japan) instrument with a validated application.

Study design

Based on previous literature, we focused on four candidate miRNAs (miR-320a, miR-483-5p, miR-1233, and miR-134) that are associated with cardiovascular and thromboembolic diseases [13, 19, 20]. We used a microarray that contained miRNAs of interest to detect their levels in 26 healthy volunteers with 20 mg rivaroxaban. Subsequently, quantitative reverse transcription polymerase chain reaction (RT-qPCR) was conducted on the same samples to exclude undetectable miRNAs. Finally, miR-320a and miR-483-5p were selected and validated by RT-qPCR in 65 healthy volunteers with 10 or 15 mg rivaroxaban and 71 patients with 15 or 20 mg rivaroxaban. Figure 1 shows a general flowchart of the study.

Since different doses and diet status affect the pharmacokinetic parameters of rivaroxaban [18], healthy volunteers were classified by dose and as fasted or fed. In the discovery phase, subjects with high or low AXA_{3h} values were classified into case and control groups, respectively. In the validation phase, the top ~40% of subjects with high AXA_{3h} or AUC_{0-t} values in each dosage group were classified as the case group, while the bottom ~40%

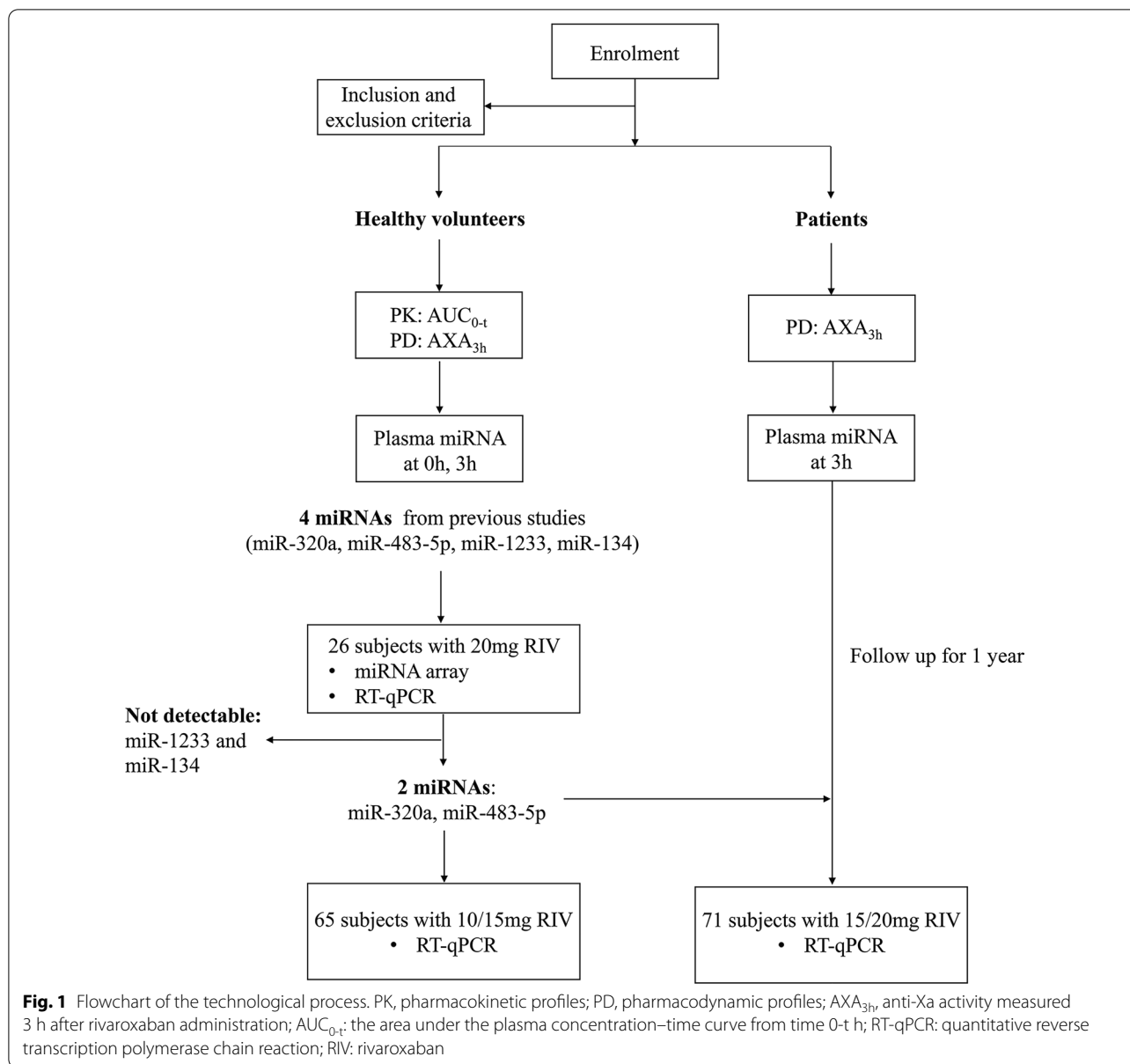
of subjects with low values were classified as the control group. The miRNAs of the subjects with relatively high or low values were compared. Patients were classified into case and control groups according to the AXA_{3h} value. The top and bottom ~20% of the patients with high or low AXA_{3h} were treated as the case and control groups, respectively. Moreover, the patients were classified according to the occurrence of bleeding events within 12 months. Case–control matching was used in patients with or without bleeding based on dose, age (± 3 years), sex, diet, indication, whether performed radiofrequency catheter ablation (RFCA), and whether combined with coronary heart disease.

miRNA microarray

Agilent miRNA array was used for the miRNA profiling in accordance with the manufacturer's instructions. Each slide of the Agilent array has eight identical arrays (8 × 60 K format), and each array contains probes that interrogates 2549 human mature miRNAs from miRBase R21.0. Each miRNA was detected by probes repeat for 30 times. 2164 Agilent control probes are also included in the array. In a nutshell, the Agilent miRNA labeling reagent was used to label the miRNAs. The labeled RNA was isolated and hybridized to miRNA arrays after being dephosphorylated and ligated with pCp-Cy3 using 200 ng of total RNA. Agilent feature extraction software version 10.10 was used to analyze the images after they had been scanned using the Agilent microarray scanner (Agilent). The GeneSpring software V13 (Agilent) was used to analyze the miRNA array data for data summarization, standardization, and quality control (Agilent).

Quantitative reverse transcription polymerase chain reaction

Total RNA was isolated from 200 μ L of plasma using the miRNeasy Serum/Plasma Advanced Kit (QIAGEN). Reverse transcription was performed using the TaqMan Advanced miRNA cDNA synthesis kit (Thermo Fisher Scientific). Subsequently, RT-qPCR reactions were performed using the predesigned TaqMan Advanced miRNA Assays (Thermo Fisher Scientific) on the StepOne Plus Real-Time PCR System (Applied Biosystems). All procedures were performed according to the manufacturer's instructions. The expression of miR-16-5p is stable according to the literature, and it is often used as an endogenous reference [21–25]. Therefore, the relative expression levels of miRNAs were normalized to has-miR-16-5p. All RT-qPCR experiments were performed in triplicate, and the mean Ct values were calculated. The relative expression of miRNA was evaluated using the comparative cycle threshold (Ct) method and reported as $2^{-\Delta Ct}$, where $\Delta Ct = \text{mean Ct}_{\text{miRNA of interest}} - \text{mean Ct}_{\text{miR-16}}$.



Bioinformatics analysis

The miRNA-predicted targets were analyzed using three different algorithms (TargetScan 8.0, miRTarBase 8.0, and miRDB 6.0) [26–28]. Only target genes validated by qPCR, western blotting, or reporter assays were included in the following analysis. Gene ontology (GO) enrichment and Kyoto Encyclopedia of Genes and Genomes (KEGG) analyses of the predicted genes were performed using Metascape (<http://metascape.org>) [29]. The default value was used as the cut-off criterion.

The miRNA–mRNA regulatory network was visualized by Cytoscape 3.7.2 [30]. The protein–protein

interaction (PPI) network of the predicted target genes of the two miRNAs was established through STRING 11.5 (Search Tool for the Retrieval of Interacting Genes database (STRING) website (<http://string-db.org>) [31]. The disconnected nodes were hidden in the network. The network was visualized by Cytoscape 3.7.2 and further analyzed using molecular complex detection (MCODE) [32] and CytoHubba [33]. The MCODE analysis is a density-based non-overlapping clustering algorithm. Hub genes were identified using CytoHubba software. All parameters of the plugin were left at their default values.

Statistical analysis

Demographic and clinical characteristics are presented as median ± interquartile range (IQR) for continuous variables and compared using the Mann–Whitney test. Categorical variables were presented using count (frequency) and tested for baseline comparability using Fisher’s exact test. Differences in miRNA levels between the case and control groups were evaluated using the Mann–Whitney unpaired test. Wilcoxon matched-pairs signed rank test was used for comparison between 0 and 3 h samples in the same group. Spearman correlation analysis was performed to describe the correlation. Univariate logistic regression analysis was performed, presenting the odds ratio (OR) and the 95% confidence interval (CI). The area under the curve (AUC) of the receiver operating characteristic curve was used to assess the predictive accuracy of miRNAs. Statistical analysis and graphics were performed using the Statistical Package for Social Sciences (SPSS version 24.0, SPSS Inc., Chicago, IL, USA) and

GraphPad Prism 9. Two-sided tests where $p < 0.05$ were considered statistically significant.

Results

Recruitment and participant characteristics

Twenty-Six healthy volunteers taking 20 mg rivaroxaban with high or low AXA_{3h} were selected for miRNA microarray analysis. RT-qPCR was conducted on the same samples. Since miR-1233 and miR-134 were not detectable in at least 90% of the individuals after RT-qPCR, we excluded these two miRNAs for further analysis, and miR-320a and miR-483-5p were used.

MiR-320a and miR-483-5p were quantified by RT-qPCR in 65 healthy volunteers (10 mg, $n = 26$; 15 mg, $n = 39$). The baseline characteristics are shown in Table 1. Significant differences in AXA_{3h} and AUC_{0-t} were observed between the case and control groups. There were no significant differences in sex, age, or body mass index (BMI) between the two groups.

Table 1 Baseline characteristics of healthy volunteers whose miRNA levels were quantified

	Total	Group classified by AXA _{3h}				Group classified by AUC _{0-t}				
		Overall	Case	Control	<i>p</i> value	Overall	Case	Control	<i>p</i> value	
10 mg										
<i>n</i>	26	20	10	10	1.000	20	10	10	1.000	
Male	15 (57.69%)	11 (55.00%)	4 (40.00%)	7 (70.00%)	0.370	12 (60.00%)	8 (80.00%)	4 (40.00%)	0.170	
Fed	13 (50.00%)	10 (50.00%)	5 (50.00%)	5 (50.00%)	1.000	10 (50.00%)	5 (50.00%)	5 (50.00%)	1.000	
Age	32 (13)	34 (16)	37.5 (16)	31.5 (14)	0.579	35.5 (15)	33 (14)	36 (14)	0.796	
BMI	23.35 (1.8)	23.35 (1.70)	23.40 (2.50)	22.60 (1.60)	0.853	23.40 (2.00)	23.10 (2.10)	23.40 (1.80)	0.912	
AXA _{3h}	134.04 (70.98)	134.58 (123.28)	195.93 (74.51)	86.28 (32.26)	0.000*	117.08 (78.49)	92.95 (35.58)	167.41 (64.05)	0.000*	
C ₃	163.1745 (108.41)	160.95 (104.41)	197.43 (85.37)	103.34 (45.57)	0.000*	146.36 (99.96)	103.34 (42.82)	194.46 (62.13)	0.000*	
C _{max}	191.9635 (69.81)	188.00 (96.67)	225.14 (78.56)	137.44 (78.92)	0.003*	187.16 (82.93)	137.44 (67.60)	215.98 (57.62)	0.001*	
AUC _{0-t}	1302.5875 (751.46)	1231.48 (780.15)	1633.65 (622.65)	910.76 (415.46)	0.000*	1350.74 (866.89)	840.75 (354.44)	1702.33 (316.65)	0.000*	
15 mg										
<i>n</i>	39	28	14	14	1.000	28	14	14	1.000	
Male	33 (84.62%)	23 (82.14%)	10 (71.43%)	13 (92.86%)	0.326	23 (82.14%)	13 (92.86%)	10 (71.43%)	0.326	
Fed	21 (53.85%)	14 (50.00%)	7 (50.00%)	7 (50.00%)	1.000	14 (50.00%)	7 (50.00%)	7 (50.00%)	1.000	
Age	29 (10)	27 (11)	24 (8)	30 (11)	0.114	25 (9)	27 (10)	24.5 (9)	0.401	
BMI	22.2 (3.2)	22.10 (2.70)	21.70 (2.30)	23.20 (2.90)	0.401	23.10 (3.30)	23.30 (3.50)	22.55 (3.40)	0.804	
AXA _{3h}	171.22 (175.59)	164.39 (219.13)	273.28 (79.31)	54.78 (113.13)	0.000*	169.96 (155.77)	93.07 (109.99)	221.93 (75.05)	0.000*	
C ₃	208 (183)	210.00 (224.25)	329.50 (75.75)	107.00 (75.75)	0.000*	203.00 (169.50)	129.00 (99.00)	277.00 (100.75)	0.000*	
C _{max}	283 (164)	284.00 (172.75)	358.50 (53.75)	196.00 (78.75)	0.000*	283.00 (136.25)	201.50 (86.25)	326.00 (86.50)	0.000*	
AUC _{0-t}	1782.71 (1212.23)	1816.22 (1123.77)	2118.18 (542.33)	1090.19 (491.24)	0.000*	1728.31 (1402.69)	1074.30 (468.58)	2440.31 (653.37)	0.000*	

Values are median (IQR), *n* (%)

IQR interquartile range; AXA_{3h} anti-Xa activity measured 3 h after rivaroxaban administration, AUC_{0-t} area under the plasma concentration time-curve from time 0 to time of last determinable concentration, BMI body mass index, C₃ plasma concentration 3 h after administration, C_{max} maximum plasma concentration

* $p < 0.05$

Table 2 Baseline characteristics of the patients

	Overall (n = 71)
Dosage	
n (15 mg)	25 (35.2%)
n (20 mg)	46 (64.8%)
Diet status (fasted/fed)	45/26
Male	35 (49.3%)
Age, years	68 (15)
BMI, kg/m ²	26.26 (4.05)
Indication	
AF	69 (97.2%)
VTE	4 (5.6%)
RFCA	35 (49.3%)
AXA _{3h}	348.66 (156.21)
Case (n = 14)	508.28 (74.05)
Control (n = 14)	202.11 (76.66)
p value	0.000*
Smoking (yes/never/cessation)	10/54/7
Comorbidity	
Diabetes	17 (23.9%)
Hyperlipemia	23 (32.4%)
Coronary heart disease	29 (40.8%)
Baseline blood tests	
HGB, g/L	133 (24)
PLT, 10 ⁹ /L	188 (65)
MPV, fL	9.1 (1.62)
Outcomes	
Any bleeding	23 (32.4%)

Values are median (IQR), n (%)

IQR interquartile range, BMI body mass index, AF atrial fibrillation, VTE venous thromboembolism, RFCA radiofrequency catheter ablation, HGB hemoglobin, PLT platelet, MPV mean platelet volume

*p < 0.05

In the patient group, miRNAs from 71 patients taking 15 or 20 mg rivaroxaban in two sub-centers were quantified. Most patients took rivaroxaban for atrial fibrillation (AF) (97.2%). 25 patients (35.2%) took 15 mg and 46 patients (64.8%) took 20 mg. There were significant differences in AXA_{3h} between the case and control groups. 23 patients suffered any bleeding events within their follow-up. Six pairs of patients were matched based on the occurrence of bleeding events within one year and demographic characteristics. The baseline characteristics of the patients are presented in Table 2.

Association between miRNAs at 3 h and rivaroxaban PK-PD profiles

Healthy volunteers with 15 mg rivaroxaban

Among the thirty-nine healthy volunteers taking 15 mg rivaroxaban whose miRNA levels were detected, AXA_{3h} was significantly positively correlated with AUC_{0-t} (r = 0.739, p = 0.000). The miR-320a level at 3 h was significantly positively correlated with AXA_{3h} and AUC_{0-t} (r = 0.359, p = 0.025; r = 0.370, p = 0.02, respectively). A positive correlation was also observed between miR-483 and AXA_{3h} or AUC_{0-t} (r = 0.372, p = 0.02; r = 0.523, p = 0.001, respectively). Figure 2 shows the correlation between these two miRNAs and AXA_{3h} (A) and AUC_{0-t} (B).

For miR-320a, there was no significant difference between the case and control groups, regardless of whether AXA_{3h} or AUC_{0-t} was used to distinguish between the two groups. No significant differences were found in the subgroups classified by diet status. For miR-483, the plasma level was significantly higher in the case group than in the control group (group

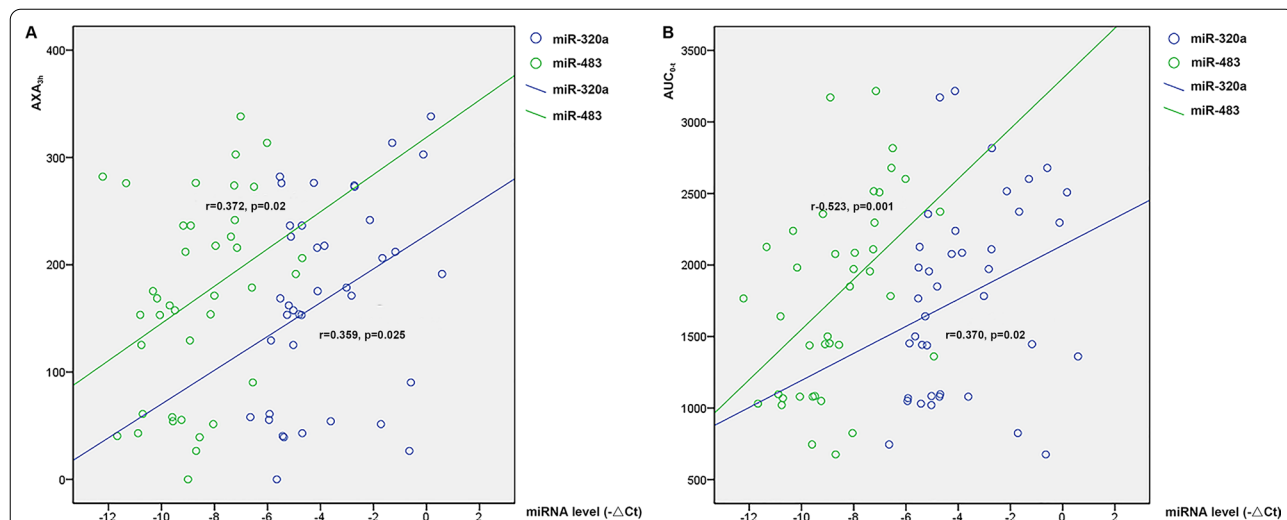


Fig. 2 Correlation between two miRNAs and AXA_{3h} (A) or AUC_{0-t} (B). AXA_{3h}, anti-Xa activity measured 3 h after rivaroxaban administration; AUC_{0-t}: the area under the plasma concentration–time curve from time 0-t h

classified by AXA_{3h} , $p=0.0310$; group classified by AUC_{0-t} , $p=0.0067$). After analysis by diet status, significant differences were found between the two fasted groups (group classified by AXA_{3h} , $p=0.0111$; group classified by AUC_{0-t} , $p=0.0379$), but no significant difference was observed in the fed group. The significant association between miRNAs at 3 h and rivaroxaban PK-PD profiles are summarized in Table 3 and Additional file 3: Table S3.

Logistic regression analysis was used to further assess the association between miRNAs and PK-PD profiles. Since miRNA levels ($2^{-\Delta Ct}$) were non-normally distributed and the clinical significance of increasing each additional unit was not clear, we scaled the two miRNAs by their respective IQR [34] to examine the effect of miRNAs on the risk for high AXA_{3h} , as estimated by odds ratios. The results showed that the miR-483 level at 3 h standardized by IQR could significantly differentiate the case and control groups classified by AXA_{3h} (OR, 5.608; 95% CI, 1.112–28.282; $p=0.037$). The same analysis was performed to identify the indicators that differentiated groups classified by AUC_{0-t} . However, miR-320a and miR-483 levels did not differ between the two groups (Additional file 4: Table S4).

To estimate the predictive value of miR-483 for indicating the rivaroxaban response, ROC curves and AUCs were calculated. In healthy volunteers taking 15 mg rivaroxaban, ROC analysis revealed an AUC of miR-483 levels (represented by $2^{-\Delta Ct}$) in the groups classified by AXA_{3h} and AUC_{0-t} of 0.740 (95% CI = 0.533–0.946; sensitivity: 71.4%; specificity: 92.9%; $p=0.031$) and 0.796 (95% CI = 0.616–0.976; sensitivity: 71.4%; specificity: 92.9%; $p=0.008$), respectively, when a cut-off value of 0.00384 was used (Fig. 3).

Healthy volunteers with 10 mg rivaroxaban

Among twenty-six healthy volunteers who took 10 mg rivaroxaban, AXA_{3h} was significantly positively correlated with AUC_{0-t} ($r=0.816$, $p=0.000$). MiR-320a and miR-483 level at 3 h were also positively correlated with AXA_{3h} and AUC_{0-t} ; however, this was not significant. In the fed subgroup, miR-320a level at 3 h in the case group (classified by AUC_{0-t}) was significantly higher than that in the control group ($p=0.0317$). MiR-483 level at 3 h in the fed case group was also significantly higher than that in the control group (group classified by AXA_{3h} , $p=0.0317$; group classified by AUC_{0-t} , $p=0.0159$), as shown in Table 3 and Additional file 3: Table S3. Odds ratio analysis showed that neither miRNA could differentiate between the two groups (Additional file 4: Table S4).

Patients with 15 or 20 mg rivaroxaban

In 71 patients, we did not find a significant association between AXA and bleeding events. For miR-320a and miR-483, the comparison between the case and control groups showed no significant differences. There was also no significant difference between the matched patients with and without bleeding (Additional file 5: Table S5). Neither miR-320a nor miR-483 was a predictive factor that could distinguish between case and control groups classified by AXA_{3h} according to odds ratio analysis. Among matched bleeding and non-bleeding patients, miR-320a and miR-483 levels could not differentiate the risk of bleeding events (Additional file 6: Table S6).

Association between miRNAs dynamics and rivaroxaban PK-PD profiles

In healthy volunteers administered 15 mg rivaroxaban, spearman correlation analysis showed that the fold

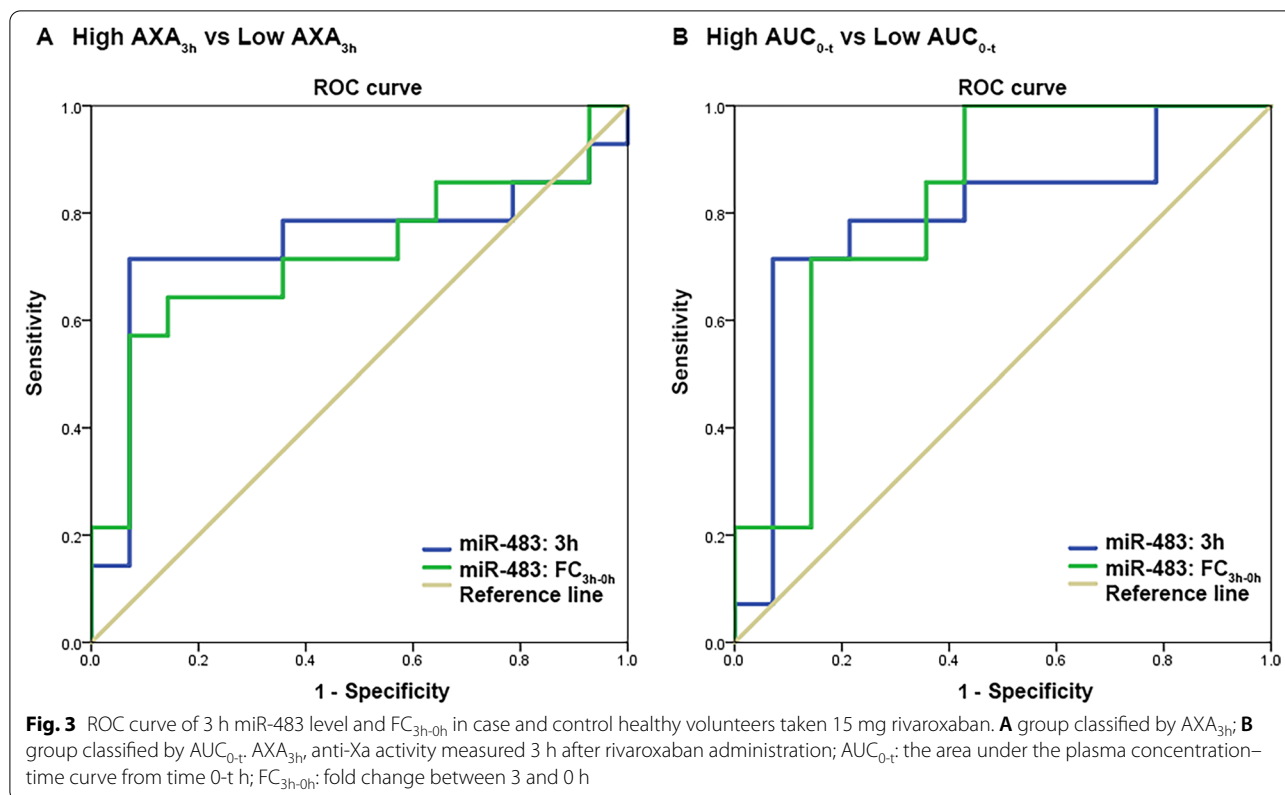
Table 3 Significant association between miRNAs at 3 h and rivaroxaban PK-PD profiles

Group criteria	Fasted	$FC_{case-control}$	p value	Fed	$FC_{case-control}$	p	Total	$FC_{case-control}$	p value
15 mg									
Grouped by AXA_{3h}									
3 h: case vs control	miR-483↑	3.38	0.0111	–	–	–	miR-483↑	2.44	0.0310
Grouped by AUC_{0-t}									
3 h: case vs control	miR-483↑	3.12	0.0379	–	–	–	miR-483↑	2.21	0.0067
10 mg									
Grouped by AXA_{3h}									
3 h: case vs control	–	–	–	miR-483↑	213.95	0.0317	–	–	–
Grouped by AUC_{0-t}									
3 h: case vs control	–	–	–	miR-320a↑	35.89	0.0317	–	–	–
3 h: case vs control	–	–	–	miR-483↑	191.69	0.0159	–	–	–

↑ indicates that this miRNA expression at 3 h was significantly higher in the case group than in the control group

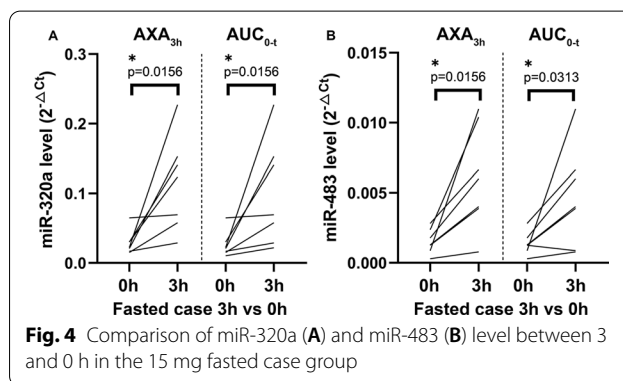
–: None

$FC_{case-control}$ fold change between case and control



change of miR-320a between 3 and 0 h (FC_{3h-0h}) was significantly positively correlated with AUC_{0-t} ($r=0.319$, $p=0.048$), and the FC_{3h-0h} of miR-483 was significantly positively correlated with AUC_{0-t} ($r=0.394$, $p=0.013$). The FC_{3h-0h} of these two miRNAs were also positively correlated with AXA_{3h} but were not statistically significant.

The miRNA levels were compared at different time points in the same group, and the miR-320a level at 3 h was significantly higher than that at 0 h in the case group (group classified by AXA_{3h} , $p=0.0085$; group classified by AUC_{0-t} , $p=0.0001$). Among fasted subjects, significant differences were also found between 3 and 0 h in the case group (group classified by AXA_{3h} , $p=0.0156$; group classified by AUC_{0-t} , $p=0.0156$) (Fig. 4A). In fed subjects, a significant difference was found between 3 and 0 h in the case group classified by AUC_{0-t} . However, no significant differences were observed in miR-320a levels between the different time points in the control group. For miR-483, the level at 3 h was significantly higher than 0 h in the case group classified by AUC_{0-t} ($p=0.0017$). When subgroup analysis was conducted in fasted subjects, significant differences were found between 3 and 0 h in the case group, regardless of the classification method used (group classified by AXA_{3h} , $p=0.0156$; group classified by AUC_{0-t} , $p=0.0313$) (Table 4, Fig. 4B). There was no



significant difference between the two time points in the control group. In healthy volunteers with 10 mg rivaroxaban, no significant differences in miR-320a or miR-483 levels were found between 3 and 0 h in the case or control group; besides, since miRNA at baseline was not collected in patients, a comparison between 3 and 0 h cannot be conducted. The associations between miRNA dynamics and rivaroxaban PK-PD profiles are summarized in Table 4 and Additional file 7: Table S7.

In healthy volunteers with 15 mg rivaroxaban, logistic regression analysis showed that miR-320a could not distinguish between the case and control groups. In the

Table 4 Association between miRNAs dynamics and rivaroxaban PK-PD profiles

Group criteria	Fasted	FC _{3h-0h}	p value	Fed	FC _{3h-0h}	p value	Total	FC _{3h-0h}	p value
15 mg									
Grouped by AXA _{3h}									
Case: 3 h vs 0 h	miR-320a↑	3.99	0.0156	–	–	–	miR-320a↑	5.47	0.0085
	miR-483↑	4.01	0.0156	–	–	–	–	–	–
Grouped by AUC _{0-t}									
Case: 3 h vs 0 h	miR-320a↑	3.86	0.0156	miR-320a↑	7.87	0.0156	miR-320a↑	6.46	0.0001
	miR-483↑	3.48	0.0313	–	–	–	miR-483↑	3.98	0.0017

↑ indicates that this miRNA expression in the case group was significantly higher at 3 h than at 0 h

–: None

FC_{3h-0h} fold change between 3 and 0 h

fasted group, FC_{3h-0h} of miR-483 may be a predictor of high or low AUC_{0-t} (OR, 6.177; 95% CI 1.04–36.696; $p=0.045$). ROC analysis showed that the AUC of FC_{3h-0h} of miR-483 in the groups classified by AXA_{3h} and AUC_{0-t} was 0.719 (95% CI=0.519–0.920; sensitivity: 64.3%; specificity: 85.7%; $p=0.048$), 0.816 (95% CI=0.652–0.981; sensitivity: 71.4%; specificity: 85.7%; $p=0.004$), respectively, when a cut-off value of 2.184 was used (Fig. 3).

In healthy volunteers with 10 mg rivaroxaban, no significant difference in miR-320a or miR-483 was found between 3 and 0 h in the case group, although an upward trend was observed (Additional file 7: Table S7).

Bioinformatics analysis for miRNA target genes and biological pathways

Three target prediction databases were used to identify the target genes of miR-320a and miR-483 (Additional file 8: Table S8). According to the miRTarBase 8.0, 34 validated genes of two miRNAs were obtained. The results showed that these miRNAs potentially regulated important genes, such as those encoding integrin subunit beta 3 (ITGB3), phosphatase and tensin homolog (PTEN), and mitogen-activated protein kinase 1/3 (MAPK1/3).

Subsequently, the validated genes were subjected to GO and KEGG analyses using Metascape. The top 20 clusters with their representative enriched terms for GO analysis are shown in Fig. 5A. The target genes of miR-320a-3p were significantly enriched in enzyme-linked receptor protein signaling pathway, regulation of MAPK cascade, regulation of cell size, cellular homeostasis, and negative regulation of cell differentiation. KEGG pathway analysis showed that the enrichment terms converged on the PI3K-Akt signaling pathway, microRNAs in cancer, transcriptional misregulation in cancer, renin secretion, and hematopoietic cell lineage, among others (Fig. 5B).

A total of 34 validated target genes targeted by two miRNAs, were selected for construction of a miRNA-mRNA network (Fig. 6A). The PPI network had 29 nodes

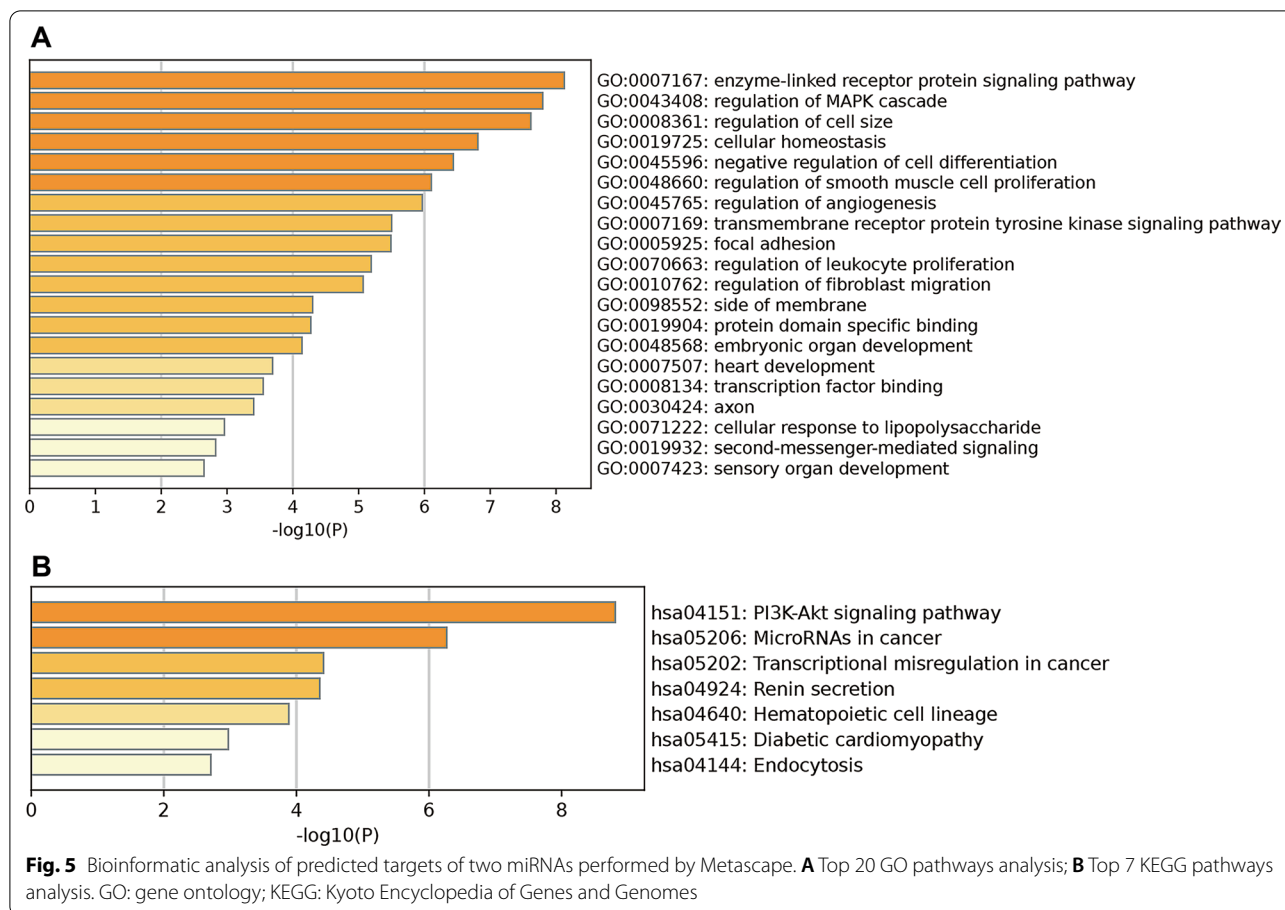
and 75 edges (Fig. 6B). We screened the top two clusters with the highest clustering scores using the MCODE plugin (Fig. 6C, D). Moreover, ten hub genes (MAPK3, MAPK1, IGF1R, PTEN, ITGB3, YWHAZ, RAC1, MCL1, KITLG, and SRF) were identified from the PPI network using the CytoHubba plugin of Cytoscape (Fig. 6E).

Discussion

To the best of our knowledge, this is the first study to assess the relationship between miRNAs and PK-PD profiles of rivaroxaban in Chinese populations, providing a model for further clinical and mechanistic research on miRNAs.

Currently, data on miRNAs influencing PK/PD and clinical outcomes of rivaroxaban application remain unclear. Only one study assessed the role of miR-142 and miR-39 for drug-monitoring of rivaroxaban among elderly patients with atrial fibrillation [35]. However, the sample size was small and AXA activity was not analyzed. Due to the insufficient information on miRNAs in Chinese populations, we discover novel miRNA biomarkers and their respective values of influence on individual anticoagulation therapy with rivaroxaban.

This study found that in healthy volunteers taking 15 mg rivaroxaban, miR-320a and miR-483 measured at 3 h post-dose were significantly positively correlated with AXA_{3h} and AUC_{0-t}. The level of miR-483 at 3 h in the case group was significantly higher than that in the control group. The miR-483 level standardized by IQR measured at 3 h was the only factor that could significantly differentiate case and control groups classified by AXA_{3h}. In addition, ROC analysis showed that miR-483 level had the potential to distinguish groups classified by AXA_{3h} or AUC_{3h}. Moreover, in the group with higher AUC_{0-t} values, miR-320a and miR-483 at 3 h were significantly higher than those at 0 h. Subgroup analysis showed that miR-320a and miR-483 at 3 h were significantly higher than that at 0 h in fasted groups with higher AXA_{3h} or



AUC_{0-t} . Additionally, ROC analysis showed that FC_{3h-0h} of miR-483 level also had the potential to distinguish groups classified by AXA_{3h} or AUC_{3h} . At a dose of 10 mg, miR-483 at 3 h was significantly higher in the fed case group than in the control group, and miR-320a expression was significantly higher in the high AUC_{0-t} group than in the low group. No significant differences were found in the other comparisons. The insignificant effect between 3 and 0 h may be due to the smaller dosage size.

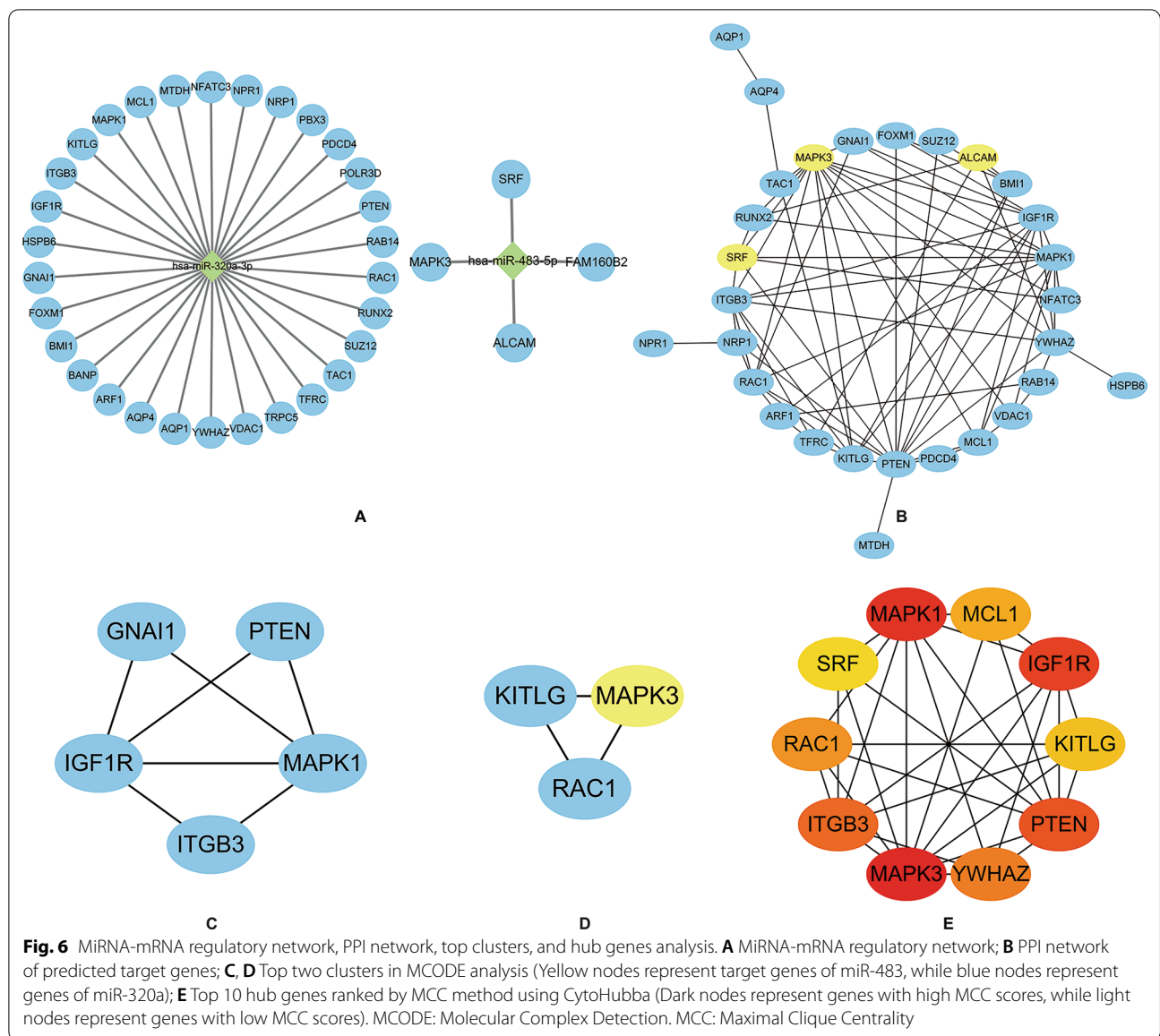
Furthermore, we measured the miRNA levels in patients. However, the results obtained in healthy people were not well validated in patients. The reasons for the failure to verify the effect of miRNAs on PD and bleeding events in patients could be as follows. First, multiple factors, including diseases, combined medication, renal impairment, hepatic impairment, age, body weight, gender, ethnicity, and diet, may influence the metabolism of the drug and these indexes are different between healthy subjects and patients. For rivaroxaban, age and renal function are most vital [6]. In this study, patients were significantly older than the healthy subjects, which may provide differences in PK profiles. Thus, the presence of a variety of confounding factors may lead to the cover-up

of miRNA effects. Second, previous clinical studies had shown a correlation between AXA and bleeding events [36, 37], whereas no significant correlation was observed in our study. Furthermore, as an exploratory study, the sample size of healthy subjects and patients was small. Therefore, results need to be verified in the well-organized study which involved more patients, and subgroup analysis may help provide more information.

Bioinformatic analysis revealed that miR-320a and miR-483 regulate different genes and are involved in different pathways. The potential mechanism regulating the PK and PD profiles of rivaroxaban is discussed here.

1. The association of miR-320a, and BCRP (gene code ABCG2)

Drug-metabolizing enzymes, transporters, nuclear receptors, and transcription factors are vital for the absorption, distribution, metabolism, and excretion (ADME) of drugs. Knowledge of the mechanisms involved in the expression and function of ADME genes is critical for predicting drug efficacy and safety profiles and lays the foundation for future precision medicine



[38–40]. Rivaroxaban, an oral, direct factor Xa inhibitor, is metabolized and excreted via CYP3A4/3A5/2J2, P-gp, and BCRP [6]. Approximately one-third of the dose is eliminated as unchanged active drug in the urine via a process thought to involve P-gp (gene code ABCB1) and BCRP (gene code ABCG2), which play important roles in the absorption of rivaroxaban, a class 2 drug according to the Biopharmaceutics Drug Disposition Classification System (BDDCS) classification system [41]. We hypothesized that miRNAs may act on transporter mRNA 3UTR or nuclear receptors, transcription factors, and other signaling molecules, which are transporter regulators.

In a previous study, miR-320a negatively regulated the expression of ABCG2 at the transcriptional level [42]. Kang et al. reported that miR-320a suppressed the promoter activity of ABCG2, but not the luciferase activity of its 3-UTR, and found that the promoter region of ABCG2 contained putative binding sites for nuclear factor of activated T cell isoform c3 (NFATc3). Thus, they speculated that miR-320a decreased the expression of ABCG2 at the transcriptional level by targeting NFATc3. In another study, miR-320a was validated to directly target the 3-UTR of NFATc3 [43]. They found that NFATc3 was essential for P-gp-induced chemoresistance. Therefore, we speculated that high levels of miR-320a reduce rivaroxaban transport activity by downregulating ABCG2

at the transcriptional level, leading to variability in PK and PD profiles (a high value of AUC_{0-t} and AXA_{3h}).

2. The association of miR-320a, miR-483 and MAPK signaling pathway

Regulation of the MAPK cascade ranks high in the GO enrichment analysis. MAPK3 and MAPK1 are both hub genes ranked by the CytoHubba plugin, and they are predicted target genes of miR-483 and miR-320a, respectively, in all three algorithms. The MAPK cascade plays a critical role in the regulation of several fundamental processes, such as proliferation, differentiation, and cell response to diverse extrinsic stresses [44]. Factor Xa is the convergence point of the extrinsic and intrinsic components of the coagulation cascade. Several studies have shown that FXa can activate MAPKs. The MAPK and NF- κ B pathways were found to be involved in FXa-induced TF expression in human umbilical endothelial cells [45]. In addition, the activation of MAPK by factor Xa leads to phosphorylation of the transcription factors that, in turn, leads to the expression of genes involved in DNA synthesis and cell proliferation [46]. FXa inhibitors may inhibit the MAPK pathway, which was previously demonstrated in the study by Hashikata et al. [47]. Thus, MAPK signaling pathways have been shown to be involved in the pathophysiology of thrombosis or platelet activity in a direct or indirect manner [48–53].

In healthy volunteers with 15 mg rivaroxaban, miR-483 levels were significantly higher in high- AXA_{3h} group, which also indicated the strong inhibition of FXa. Therefore, we speculated that the MAPK pathway was inhibited. We also found that miR-483 and miR-320a levels in the case group (a better response) measured 3 h after rivaroxaban administration was significantly higher than at baseline. MiR-483 levels also have the potential to differentiate AXA_{3h} . We assume that higher miR-483 may lead to downregulation of its predicted target gene (MAPK3), thereby inhibiting the MAPK pathway, which may inhibit thrombosis directly or indirectly. Rivaroxaban, an FXa inhibitor, may also inhibit the MAPK pathway, resulting in an enhanced antithrombotic effect at the same time. The source of increased miRNA levels and their mechanisms correlated with PK/PD profiles requires further research.

3. The association of miR-320a and integrin subunit beta 3 (ITGB3)

Previous studies have validated that ITGB3 is the target gene of miR-320a [54, 55]. It was also in the top cluster in the MCODE analysis and a hub gene ranked by the CytoHubba plugin. Fager et al. found that platelets capable

of binding FXa demonstrated significantly increased expression of key adhesion molecules, including integrin β 3, thereby placing these platelets in a unique position to contribute to both hemostatic and thrombotic events [56]. Therefore, we assumed that the upward miR-320a level may down-regulate integrin β 3 and may affect the adherent properties of platelets and their procoagulant response, which may lead to an enhanced antithrombotic effect of rivaroxaban.

Previous studies have reported that miR-320a and miR-483 are associated with atrial fibrillation or thrombotic disease. Circulating extracellular miR-320a-3p was elevated in paroxysmal AF patients compared to healthy controls and hypertensive patients without AF [57], and circulating miRNA-320a/b was differentially expressed in patients with deep vein thrombosis [58]. Elevated serum miR-483-5p levels may predict patients at risk for post-operative AF [20]. Since the level of miRNAs may also be regulated by disease status, the findings on healthy volunteers should be further validated in a larger patient cohort. The possible roles and mechanisms of these differentially expressed miRNAs should be further elucidated in patients taking rivaroxaban.

Above all, the goal of this study is to identify miRNA's potential as a biomarker for rivaroxaban therapeutic drug monitoring. The close correlation between miRNA and PK/PD parameters is the basis for this possibility. Differences in miRNA levels may influence the efficacy and safety after rivaroxaban therapy, which is particularly essential in critical situations, such as in patients with severe bleeding, for the detection of residual anticoagulant drug effects before surgery, prior to thrombolysis in acute stroke patients, after rescue from overdose, during the therapy in patients with extremes of body weight, to evaluate drug interactions, in cases of renal impairment, and in situations where there is a suspicion of non-compliance [59, 60]. Therefore, it is of great importance to discover novel biomarkers which could help distinguish subjects with different drug responses. According to our study, the likelihood that the effect of rivaroxaban is enhanced depending on the levels of miR-320a and miR-483 after administration. Given the potential link between AXA and bleeding incidents, it is also plausible that the higher miRNA levels may be associated with bleeding incidents. Therefore, in patients with higher miR-320a and miR-483 levels, particular attention should be paid to while using rivaroxaban. They may also become potential targets for rivaroxaban therapy to predict responses and help personalize pharmacotherapy.

Our study also had some limitations. First, although this study included healthy volunteers in three sub-centers, the number of subjects for microarray and RT-qPCR was still relatively small. miRNA levels in patients

with and without bleeding were only compared in six matched pairs. The number of patients was too small to draw robust conclusions. Therefore, further evidence to verify the present findings is needed. Second, although miRNAs have the potential to predict several diseases, inconsistencies among detection devices and different procedures of data acquisition (such as various normalization methods for circulating miRNAs) hinder the wide use of miRNAs for clinical applications [61]. A previous study reported that repetitive freeze–thaw cycles may result in a significant reduction in miRNA concentration in both plasma and serum samples [62]. Thus, the methodological standards for quantifying miRNAs need to be further unified and improved so that the results can be interpreted accurately. Moreover, although pathway enrichment analysis has been frequently utilized to elucidate functional implications for dysregulated circulating miRNAs, this methodology cannot be free from inherent information bias and may provide inaccurate results [63]. The precise mechanism remains unknown. Further supporting data with experimental approaches will be necessary to verify the findings of our study.

Conclusion

In conclusion, we found that miRNA impact the PK and PD profiles of rivaroxaban in healthy Chinese populations. MiR-320a and miR-483 may be novel biomarkers and potential targets for anticoagulation therapy involving rivaroxaban. Bioinformatic analysis showed that these miRNAs may play a regulatory role by targeting ABCG2, ITGB3, MAPK1/3, etc. However, no significant differences were found in the comparisons among patients. Further data are warranted to strengthen the robustness of the present findings and to analyze the role of miRNAs in predicting the PK or PD profiles and clinical outcomes of anticoagulants.

Supplementary Information

The online version contains supplementary material available at <https://doi.org/10.1186/s40246-022-00445-5>.

Additional file 1. Table S1: The inclusion criteria of healthy volunteers and patients

Additional file 2. Table S2: Analytics for the assessment of rivaroxaban plasma concentrations in healthy volunteers in sub-centers

Additional file 3. Table S3: Comparison of plasma miR-320a and miR-483 levels between the case and control groups in healthy volunteers

Additional file 4. Table S4: Risk estimates of 3 h miRNA levels for rivaroxaban response by univariate logistic analysis in healthy volunteers

Additional file 5. Table S5: Plasma miR320a/miR-483 levels compared between different groups in patients

Additional file 6. Table S6: Risk estimates of 3 h miRNA levels for rivaroxaban response by univariate logistic analysis in patients

Additional file 7. Table S7: Comparison of plasma miR-320a and miR-483 levels between 3 and 0 h in healthy volunteers

Additional file 8. Table S8: Target analysis for miR-320a and miR-483

Acknowledgements

We thank contributions of all investigators in sub-centers for this study.

Author contributions

H.Z. wrote the manuscript. Y.C. and Q.X. designed the research. H.Z., Z.Z., Z.L., G.M., Q.X., S.Z., Z.W., Y.C., Y.T., X.W., D.Y. performed the research. H.Z. and Q.X. analyzed data. All authors reviewed the manuscript. All authors read and approved the final manuscript.

Funding

This study was supported by grants from the National Key R&D Program of China (No. 2016YFC0904900), National Science and Technology Major Projects for “Major New Drugs Innovation and Development” of China (No. 2017ZX09304028), National Natural Science Foundation of China (Nos. 81872940, 81973395 and 82073935).

Availability of data and materials

All data generated or analysed during this study are included in this published article and its additional files.

Declarations

Ethics approval and consent to participate

The protocol was approved by an independent ethics committee and the Institutional Review Board of Peking University First Hospital and all participating research subcentral hospitals. The trial registration number is NCT03161496. All subjects were enrolled in this study after signing informed consent.

Consent for publication

All authors of this paper consent for publishing the manuscript and figures in the journal.

Competing interests

The authors declare that they have no competing interests.

Author details

¹Department of Pharmacy, Peking University First Hospital, No. 8, Xishiku Street, Xicheng District, Beijing 100034, China. ²School of Pharmaceutical Sciences, Peking University Health Science Center, Beijing, China. ³Office of Drug Clinical Trial Management, Affiliated Hospital of Qingdao University, Qingdao, Shandong, China. ⁴Psychiatry Research Center, Beijing HuiLongGuan Hospital, Peking University, Beijing, China. ⁵Clinical Trial Research Center, Department of Pharmacy, The First Affiliated Hospital of Nanchang University, Nanchang, Jiangxi, China. ⁶Department of Pharmacy, The 7th People's Hospital of Zhengzhou, Zhengzhou, Henan, China. ⁷Institute of Clinical Pharmacology, Peking University, Beijing, China.

Received: 27 March 2022 Accepted: 15 December 2022

Published online: 28 December 2022

References

- Weitz JI, Eikelboom JW, Samama MM. New antithrombotic drugs: Antithrombotic Therapy and Prevention of Thrombosis, 9th ed: American College of Chest Physicians Evidence-Based Clinical Practice Guidelines. *Chest*. 2012;141(2 Suppl):e120S–e51S.
- Ageno W, Gallus AS, Wittkowsky A, Crowther M, Hylek EM, Palareti G. Oral anticoagulant therapy: Antithrombotic Therapy and Prevention of Thrombosis, 9th ed: American College of Chest Physicians Evidence-Based Clinical Practice Guidelines. *Chest*. 2012;141(2 Suppl):e44S–e88S.

3. Janssen Pharmaceuticals, Inc. Xarelto (rivaroxaban) Prescribing Information. 2021. https://www.accessdata.fda.gov/drugsatfda_docs/label/2021/022406s036,202439s036lbl.pdf. Accessed 31 Aug 2021.
4. Kubitzka D, Becka M, Voith B, Zuehlsdorf M, Wensing G. Safety, pharmacodynamics, and pharmacokinetics of single doses of BAY 59–7939, an oral, direct factor Xa inhibitor. *Clin Pharmacol Ther.* 2005;78:412–21.
5. Kubitzka D, Becka M, Wensing G, Voith B, Zuehlsdorf M. Safety, pharmacodynamics, and pharmacokinetics of BAY 59–7939—an oral, direct Factor Xa inhibitor—after multiple dosing in healthy male subjects. *Eur J Clin Pharmacol.* 2005;61:873–80.
6. Mueck W, Stampfuss J, Kubitzka D, Becka M. Clinical pharmacokinetic and pharmacodynamic profile of rivaroxaban. *Clin Pharmacokinet.* 2014;53:1–16.
7. Samama MM. Which test to use to measure the anticoagulant effect of rivaroxaban: the anti-factor Xa assay. *J Thromb Haemost: JTH.* 2013;11:579–80.
8. Mueck W, Becka M, Kubitzka D, Voith B, Zuehlsdorf M. Population model of the pharmacokinetics and pharmacodynamics of rivaroxaban: an oral, direct factor xa inhibitor—in healthy subjects. *Int J Clin Pharmacol Ther.* 2007;45:335–44.
9. Testa S, Tripodi A, Legnani C, Pengo V, Abbate R, Dellanoce C, et al. Plasma levels of direct oral anticoagulants in real life patients with atrial fibrillation: results observed in four anticoagulation clinics. *Thromb Res.* 2016;137:178–83.
10. Shnayder NA, Petrova MM, Shesternya PA, Savinova AV, Bochanova EN, Zimnitskaya OV, et al. Using pharmacogenetics of direct oral anticoagulants to predict changes in their pharmacokinetics and the risk of adverse drug reactions. *Biomedicines.* 2021;9.
11. Xu J, Zhao J, Evan G, Xiao C, Cheng Y, Xiao J. Circulating microRNAs: novel biomarkers for cardiovascular diseases. *J Mol Med (Berlin).* 2012;90:865–75.
12. Eulalio A, Huntzinger E, Izaurralde E. Getting to the root of miRNA-mediated gene silencing. *Cell.* 2008;132:9–14.
13. Hembrom AA, Srivastava S, Garg I, Kumar B. MicroRNAs in venous thrombo-embolism. *Clin Chim Acta.* 2020;504:66–72.
14. Komal S, Yin JJ, Wang SH, Huang CZ, Tao HL, Dong JZ, et al. MicroRNAs: emerging biomarkers for atrial fibrillation. *J Cardiol.* 2019;74:475–82.
15. Creemers EE, Tijssen AJ, Pinto YM. Circulating microRNAs: novel biomarkers and extracellular communicators in cardiovascular disease? *Circ Res.* 2012;110:483–95.
16. Ikemura K, Iwamoto T, Okuda M. MicroRNAs as regulators of drug transporters, drug-metabolizing enzymes, and tight junctions: implication for intestinal barrier function. *Pharmacol Ther.* 2014;143:217–24.
17. Yu AM. Role of microRNAs in the regulation of drug metabolism and disposition. *Expert Opin Drug Metab Toxicol.* 2009;5:1513–28.
18. Janssen Pharmaceuticals, Inc. XARELTO® (rivaroxaban) tablets, for oral use [package insert]. 2021. https://www.accessdata.fda.gov/drugsatfda_docs/label/2021/202439_S035_022406S037lbl.pdf. Accessed 4 Oct 2021.
19. Xiang Q, Zhang HX, Wang Z, Liu ZY, Xie QF, Hu K, et al. The predictive value of circulating microRNAs for venous thromboembolism diagnosis: a systematic review and diagnostic meta-analysis. *Thromb Res.* 2019;181:127–34.
20. Harling L, Lambert J, Ashrafian H, Darzi A, Gooderham NJ, Athanasiou T. Elevated serum microRNA 483–5p levels may predict patients at risk of post-operative atrial fibrillation. *Eur J Cardiothorac Surg.* 2017;51:73–8.
21. Xiang M, Zeng Y, Yang R, Xu H, Chen Z, Zhong J, et al. U6 is not a suitable endogenous control for the quantification of circulating microRNAs. *Biochem Biophys Res Commun.* 2014;454:210–4.
22. Lawrie CH, Gal S, Dunlop HM, Pushkaran B, Liggins AP, Pulford K, et al. Detection of elevated levels of tumour-associated microRNAs in serum of patients with diffuse large B-cell lymphoma. *Br J Haematol.* 2008;141:672–5.
23. Huang Z, Huang D, Ni S, Peng Z, Sheng W, Du X. Plasma microRNAs are promising novel biomarkers for early detection of colorectal cancer. *Int J Cancer.* 2010;127:118–26.
24. Wong TS, Liu XB, Wong BY, Ng RW, Yuen AP, Wei WI. Mature miR-184 as potential oncogenic microRNA of squamous cell carcinoma of tongue. *Clin Cancer Res.* 2008;14:2588–92.
25. Redova M, Poprach A, Nekvindova J, Iliev R, Radova L, Lakomy R, et al. Circulating miR-378 and miR-451 in serum are potential biomarkers for renal cell carcinoma. *J Transl Med.* 2012;10:55.
26. McGeary SE, Lin KS, Shi CY, Pham TM, Bisaria N, Kelley GM, et al. The biochemical basis of microRNA targeting efficacy. *Science.* 2019;366.
27. Huang HY, Lin YC, Li J, Huang KY, Shrestha S, Hong HC, et al. miRTarBase 2020: updates to the experimentally validated microRNA-target interaction database. *Nucleic Acids Res.* 2020;48:D148–54.
28. Chen Y, Wang X. miRDB: an online database for prediction of functional microRNA targets. *Nucleic Acids Res.* 2020;48:D127–31.
29. Zhou Y, Zhou B, Pache L, Chang M, Khodabakhshi AH, Tanaseichuk O, et al. Metascape provides a biologist-oriented resource for the analysis of systems-level datasets. *Nat Commun.* 2019;10:1523.
30. Shannon P, Markiel A, Ozier O, Baliga NS, Wang JT, Ramage D, et al. Cytoscape: a software environment for integrated models of biomolecular interaction networks. *Genome Res.* 2003;13:2498–504.
31. Szklarczyk D, Gable AL, Nastou KC, Lyon D, Kirsch R, Pyysalo S, et al. The STRING database in 2021: customizable protein-protein networks, and functional characterization of user-uploaded gene/measurement sets. *Nucleic Acids Res.* 2021;49:D605–12.
32. Bader GD, Hogue CW. An automated method for finding molecular complexes in large protein interaction networks. *BMC Bioinform.* 2003;4:2.
33. Chin CH, Chen SH, Wu HH, Ho CW, Ko MT, Lin CY. cytoHubba: identifying hub objects and sub-networks from complex interactome. *BMC Syst Biol.* 2014;8 Suppl 4(Suppl 4):S11.
34. Berg K, Romer Present P, Richardson K. Long-term air pollution and other risk factors associated with COVID-19 at the census tract level in Colorado. *Environ Pollut.* 2021;287:117584.
35. Rytkin E, Bure IV, Bochkov PO, Akmalova KA, Mirzaev KB, Cherniaeva MS, et al. MicroRNAs as novel biomarkers for rivaroxaban therapeutic drug monitoring. *Drug Metab Personal Ther.* 2021;37:41–6.
36. Wada S, Toyoda K, Sato S, Matsuki T, Okata T, Kumamoto M, et al. Anti-Xa activity and event risk in patients with direct factor Xa inhibitors initiated early after stroke. *Circ J.* 2018;82:2872–9.
37. Testa S, Legnani C, Antonucci E, Paoletti O, Dellanoce C, Cosmi B, et al. Drug levels and bleeding complications in atrial fibrillation patients treated with direct oral anticoagulants. *J Thromb Haemost: JTH.* 2019;17:1064–72.
38. Lu AY. Drug-metabolism research challenges in the new millennium: individual variability in drug therapy and drug safety. *Drug Metab Dispos.* 1998;26:1217–22.
39. Yu AM, Pan YZ. Noncoding microRNAs: small RNAs play a big role in regulation of ADME? *Acta Pharm Sin B.* 2012;2:93–101.
40. Manikandan P, Nagini S. Cytochrome P450 structure, function and clinical significance: a review. *Curr Drug Targets.* 2018;19:38–54.
41. Shugarts S, Benet LZ. The role of transporters in the pharmacokinetics of orally administered drugs. *Pharm Res.* 2009;26:2039–54.
42. Kang DW, Yang ES, Noh YN, Hwang WC, Jo SY, Suh YA, et al. MicroRNA-320a and microRNA-4496 attenuate *Helicobacter pylori* cytotoxin-associated gene A (CagA)-induced cancer-initiating potential and chemoresistance by targeting beta-catenin and ATP-binding cassette, subfamily G, member 2. *J Pathol.* 2017;241:614–25.
43. He DX, Gu XT, Jiang L, Jin J, Ma X. A methylation-based regulatory network for microRNA 320a in chemoresistant breast cancer. *Mol Pharmacol.* 2014;86:536–47.
44. Guo YJ, Pan WW, Liu SB, Shen ZF, Xu Y, Hu LL. ERK/MAPK signalling pathway and tumorigenesis. *Exp Ther Med.* 2020;19:1997–2007.
45. Jiang R, Wang NP, Tanaka KA, Levy JH, Guyton RA, Zhao ZQ, et al. Factor Xa induces tissue factor expression in endothelial cells by P44/42 MAPK and NF-kappaB-dependent pathways. *J Surg Res.* 2011;169:319–27.
46. Ko FN, Yang YC, Huang SC, Ou JT. Coagulation factor Xa stimulates platelet-derived growth factor release and mitogenesis in cultured vascular smooth muscle cells of rat. *J Clin Invest.* 1996;98:1493–501.
47. Hashikata T, Yamaoka-Tojo M, Namba S, Kitasato L, Kameda R, Murakami M, et al. Rivaroxaban inhibits angiotensin II-induced activation in cultured mouse cardiac fibroblasts through the modulation of NF-kappaB pathway. *Int Heart J.* 2015;56:544–50.
48. Memon AA, Sundquist K, Wang X, Svensson PJ, Sundquist J, Zoller B. Transforming growth factor (TGF)-beta levels and unprovoked recurrent venous thromboembolism. *J Thromb Thrombolysis.* 2014;38:348–54.

49. Shetty S, Kulkarni B, Pai N, Mukundan P, Kasatkar P, Ghosh K. JAK2 mutations across a spectrum of venous thrombosis cases. *Am J Clin Pathol*. 2010;134:82–5.
50. Stefanini L, Bergmeier W. RAP1-GTPase signaling and platelet function. *J Mol Med (Berlin)*. 2016;94:13–9.
51. Guidetti GF, Canobbio I, Torti M. PI3K/Akt in platelet integrin signaling and implications in thrombosis. *Adv Biol Regul*. 2015;59:36–52.
52. Severin S, Ghevaert C, Mazharian A. The mitogen-activated protein kinase signaling pathways: role in megakaryocyte differentiation. *J Thromb Haemost: JTH*. 2010;8:17–26.
53. Lim CS, Kiriakidis S, Sandison A, Paleolog EM, Davies AH. Hypoxia-inducible factor pathway and diseases of the vascular wall. *J Vasc Surg*. 2013;58:219–30.
54. Sun L, Liu B, Lin Z, Yao Y, Chen Y, Li Y, et al. MiR-320a acts as a prognostic factor and Inhibits metastasis of salivary adenoid cystic carcinoma by targeting ITGB3. *Mol Cancer*. 2015;14:96.
55. Shang C, Zhang H, Guo Y, Hong Y, Liu Y, Xue Y. MiR-320a down-regulation mediates bladder carcinoma invasion by targeting ITGB3. *Mol Biol Rep*. 2014;41:2521–7.
56. Fager AM, Wood JP, Bouchard BA, Feng P, Tracy PB. Properties of procoagulant platelets: defining and characterizing the subpopulation binding a functional prothrombinase. *Arterioscler Thromb Vasc Biol*. 2010;30:2400–7.
57. Zhelankin AV, Vasiliev SV, Stonogina DA, Babalyan KA, Sharova EI, Doludin YV, et al. Elevated plasma levels of circulating extracellular miR-320a-3p in patients with paroxysmal atrial fibrillation. *Int J Mol Sci*. 2020;21.
58. Jiang Z, Ma J, Wang Q, Wu F, Ping J, Ming L. Combination of circulating miRNA-320a/b and D-Dimer improves diagnostic accuracy in deep vein thrombosis patients. *Med Sci Monit*. 2018;24:2031–7.
59. Samuelson BT, Cuker A, Siegal DM, Crowther M, Garcia DA. Laboratory assessment of the anticoagulant activity of direct oral anticoagulants: a systematic review. *Chest*. 2017;151:127–38.
60. Martin K, Moll S. Direct oral anticoagulant drug level testing in clinical practice: a single institution experience. *Thromb Res*. 2016;143:40–4.
61. Matsuzaki J, Ochiya T. Circulating microRNAs and extracellular vesicles as potential cancer biomarkers: a systematic review. *Int J Clin Oncol*. 2017;22:413–20.
62. Glinge C, Clauss S, Boddum K, Jabbari R, Jabbari J, Risgaard B, et al. Stability of circulating blood-based microRNAs—pre-analytic methodological considerations. *PLoS ONE*. 2017;12:e0167969.
63. Godard P, van Eyll J. Pathway analysis from lists of microRNAs: common pitfalls and alternative strategy. *Nucleic Acids Res*. 2015;43:3490–7.

Publisher's Note

Springer Nature remains neutral with regard to jurisdictional claims in published maps and institutional affiliations.

Ready to submit your research? Choose BMC and benefit from:

- fast, convenient online submission
- thorough peer review by experienced researchers in your field
- rapid publication on acceptance
- support for research data, including large and complex data types
- gold Open Access which fosters wider collaboration and increased citations
- maximum visibility for your research: over 100M website views per year

At BMC, research is always in progress.

Learn more biomedcentral.com/submissions

